Supporting Information

Super-Additive Interaction of Homo- and Heterosynaptic Plasticity in Hot Electron Transfer Optosynapse for Visual Sensing Memory and Logic Operation

*Li-Chung Shih, Kuan-Ting Chen, Shi-Cheng Mao, Ya-Chi Huang, Fang-Jui Chu, Tzu-Hsiang Liu, Wen-Hui Cheng, and Jen-Sue Chen**

Department of Materials Science and Engineering, National Cheng Kung University, Tainan 70101, Taiwan.

E-mail: jenschen@ncku.edu.tw

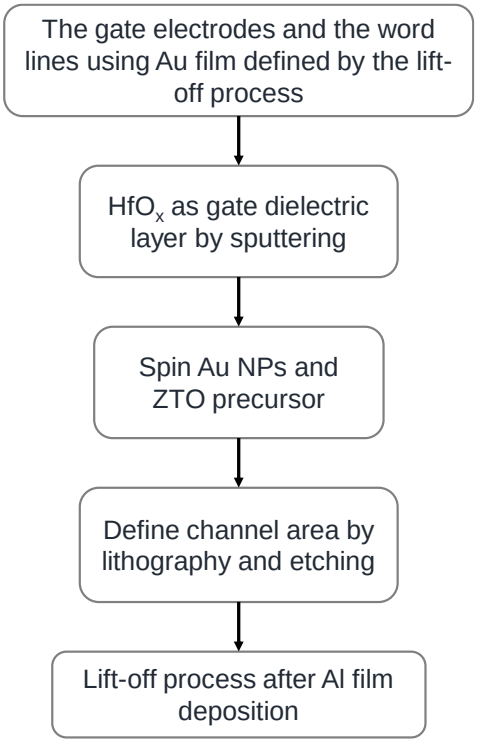

Figure S1. The proposed process flow of a large ZTO/Au NPs optosynapse array. First, the lift-off process is carried out to define both the gate electrodes and the word lines using the sputter-deposited Au films. The gate electrodes within the same row are connected to a word line. As a gate insulator, HfO_x can be deposited by sputtering. Subsequently, the Au NPs precursor is spin-coated on the gate insulator, followed by the spin-coated ZTO active layer. The photolithography and etching processes are again needed to define the channel area. Finally, the lift-off process is performed to define the drain and source lines, followed by the deposition of Al film using electron beam evaporation. The drain electrodes within each column are connected to a bit line, while the source electrodes are connected to a source line.

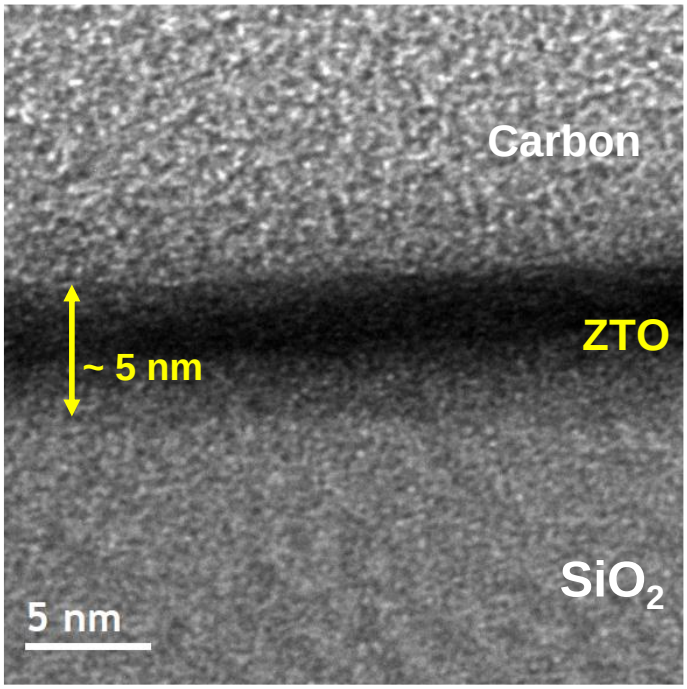

Figure S2. Cross-sectional HRTEM image of spin-coated ZTO on a SiO_2/p^+-Si substrate.

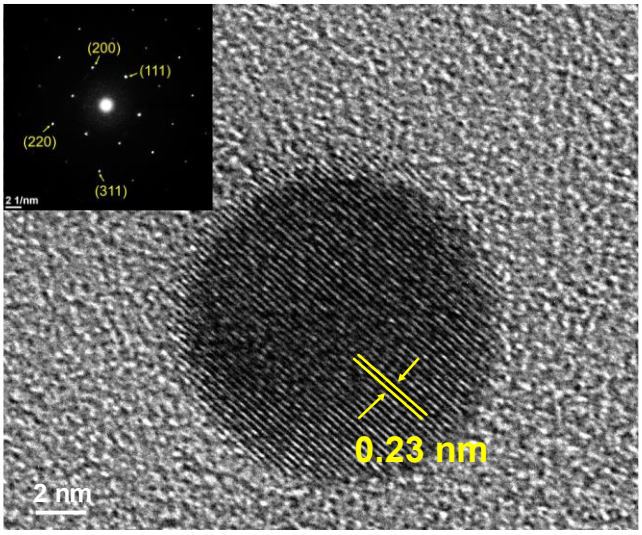

Figure S3. HRTEM image of Au NP on a SiO_2/p^+-Si substrate. The lattice spacing of Au NP is ~0.23 nm. (Inset: the nano-beam electron diffraction (NBED) pattern of Au NP)

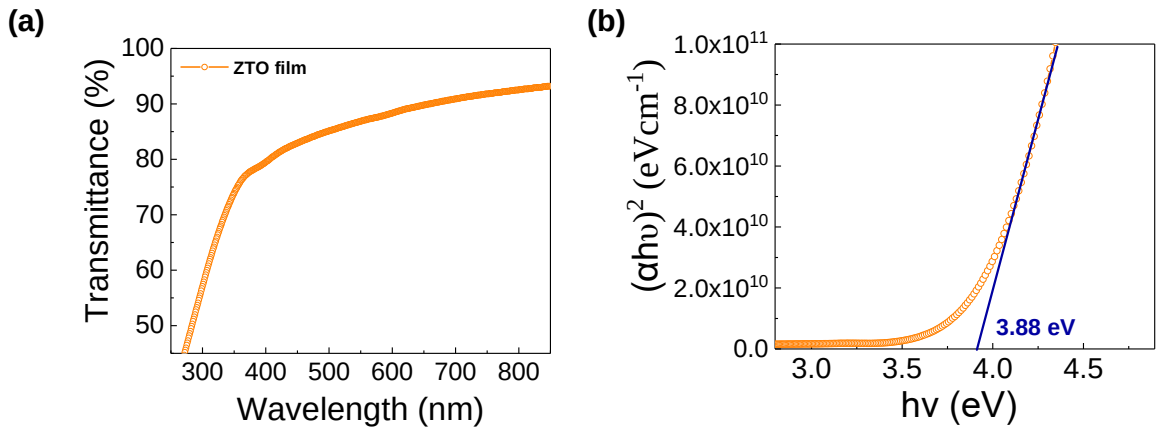

Figure S4. (a) The UV-Vis transmittance spectrum of ZTO on the quartz. (b) The corresponding plot of $(\alpha h\upsilon)^2$ as a function of photon energy for the determination of the optical bandgap of ZTO.

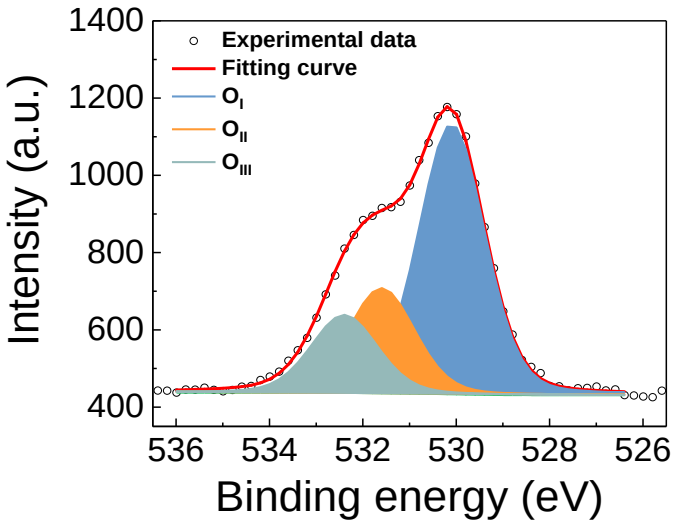

Figure S5. Deconvoluted O1s XPS spectra of ZTO deposited on the SiO_2/p^+-Si substrate.

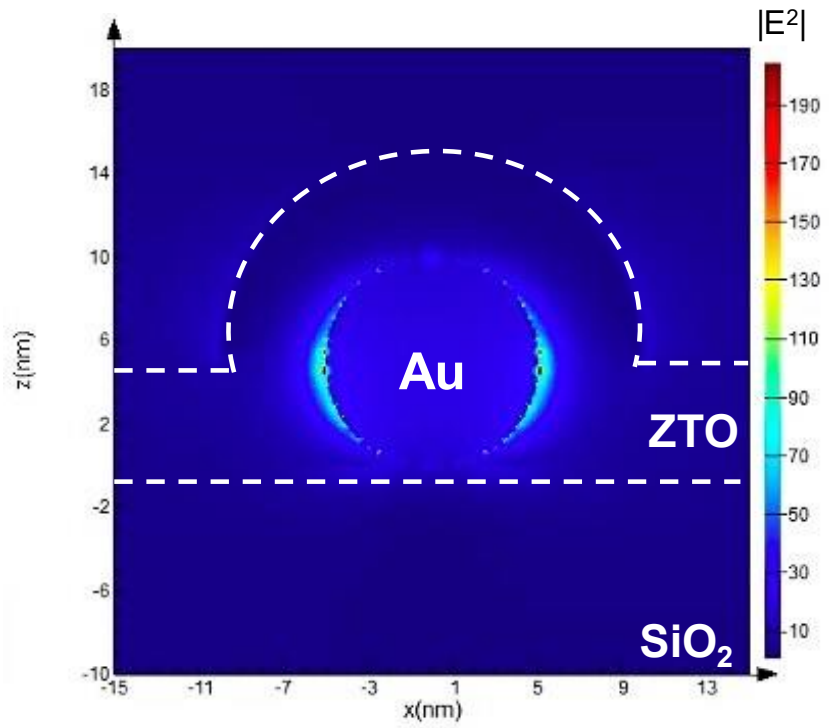

Figure S6. FDTD simulation of the electrical field intensity distribution for the ZTO/Au NP heterostructure under 545 nm light illumination.

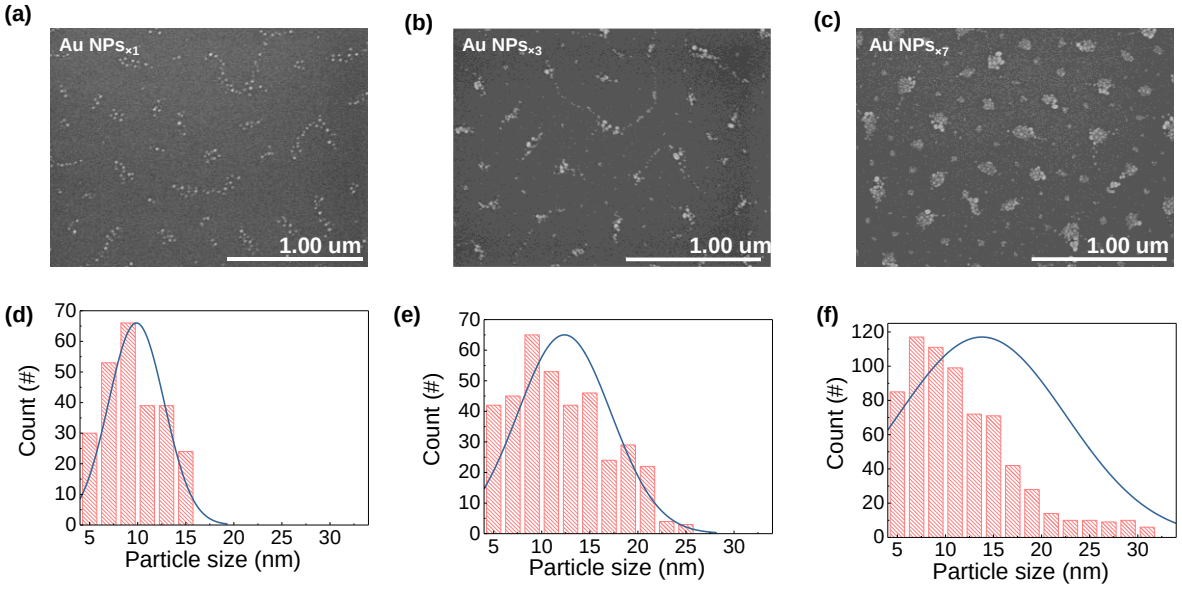

Figure S7. SEM image and particle size distribution histogram of (a)(d) Au NPs$_{\times 1}$, (b)(e) Au NPs$_{\times 3}$, and (c)(f) Au NPs$_{\times 7}$ on the SiO_2/p^+-Si substrate.

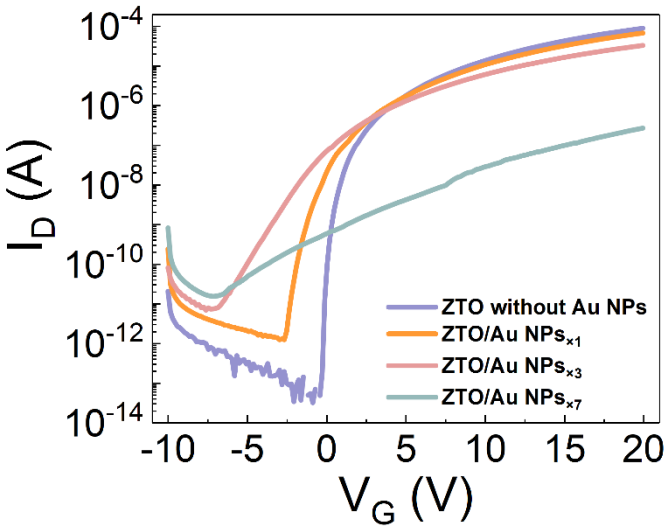

Figure S8. I_D-V_G transfer characteristics of ZTO, ZTO/Au NPs×1, ZTO/Au NPs×3, and ZTO/Au NPs×7 phototransistors measured in the dark with V_D = 10 V.

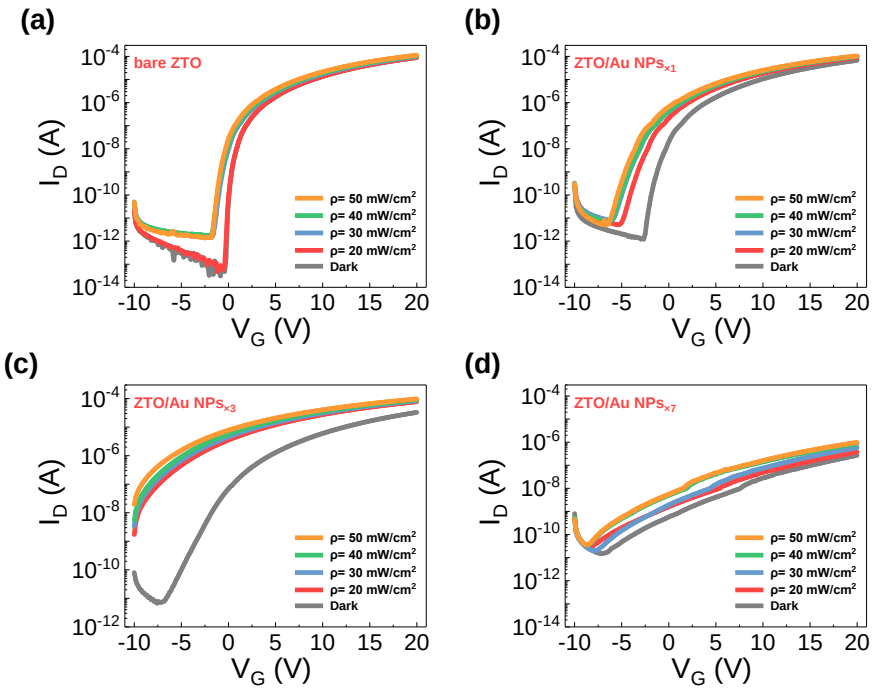

Figure S9. I_D-V_G transfer characteristics of (a) ZTO, (b) ZTO/Au NPs$_{\times 1}$, (c) ZTO/Au NPs$_{\times 3}$, and (d) ZTO/Au NPs$_{\times 7}$ phototransistors measured under 520 nm light illumination with various optical power densities. The drain voltage (V_D) is 10 V for all phototransistors.

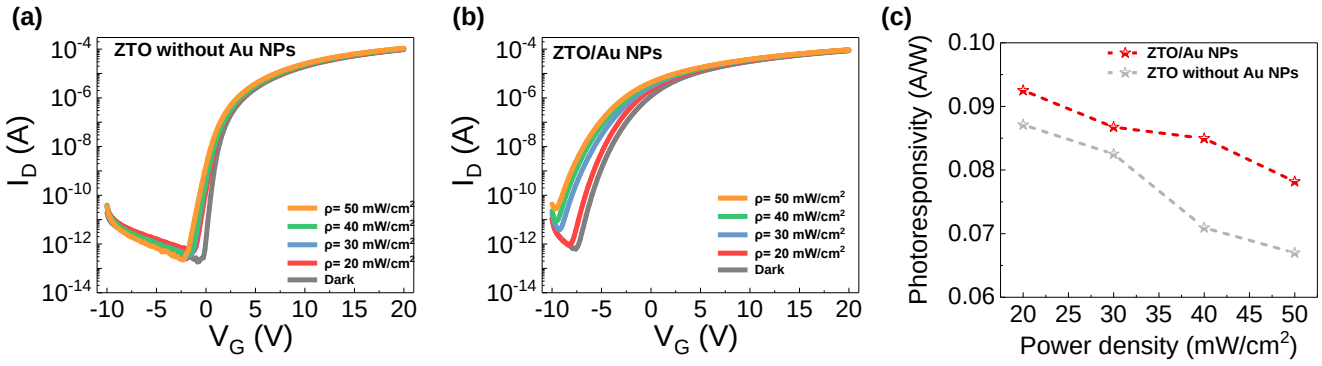

Figure S10. I_D-V_G transfer characteristics of (a) ZTO and (b) ZTO/Au NPs phototransistors measured under 635 nm light illumination with various optical power densities. The drain voltage (V_D) is 10 V for both phototransistors. (c) The extracted photoresponsivity at V_G = 20 V of ZTO and ZTO/Au NPs phototransistors to 635 nm light.

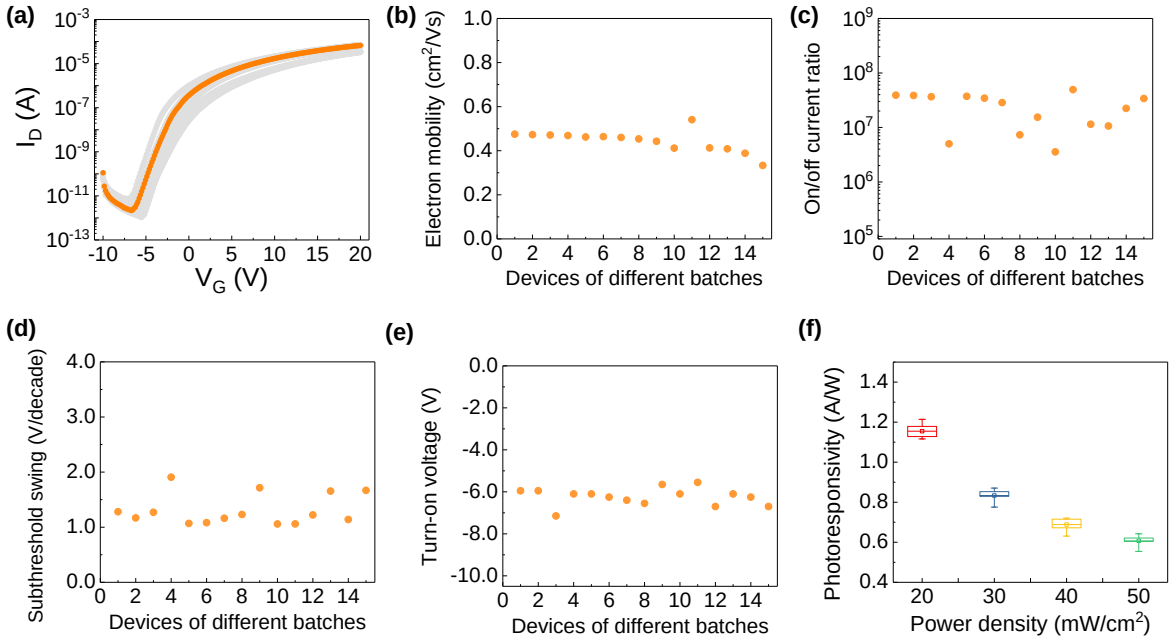

Figure S11. (a) I_D-V_G transfer characteristics of the ZTO/Au NPs$_{\times 3}$ phototransistor of different batches. (b)-(f) Statistical data for electron mobility, on/off current ratio, S.S., and V_{on} measured in the dark, as well as the photoresponsivity to 520 nm light for the ZTO/Au NPs$_{\times 3}$ phototransistors. The statistical analysis is shown in Table S1 and S2.

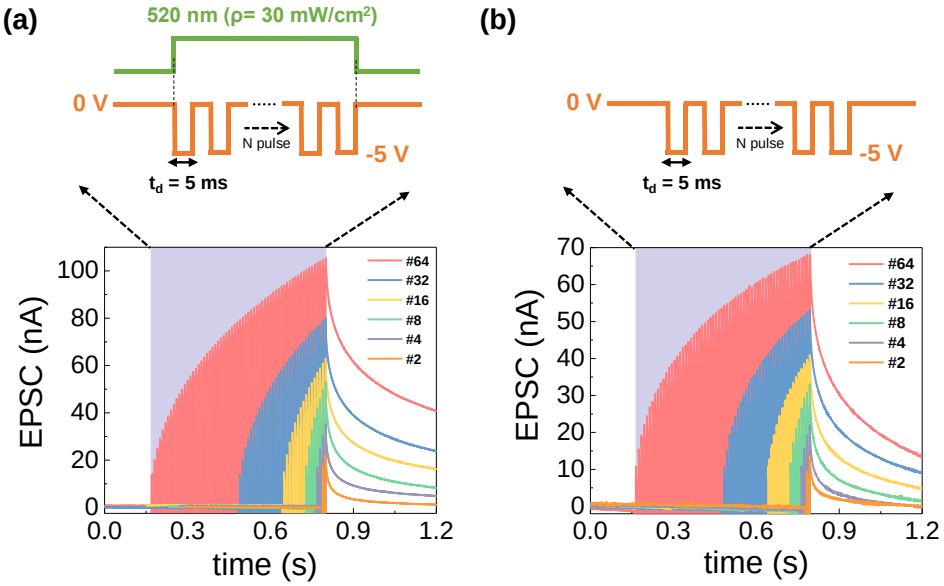

Figure S12. SNDP of the ZTO/Au NPs optosynaptic transistor with the application of voltage spikes (V_G = -5 V, t_d = 5 ms, 10 ms period) (a) under 520 nm light illumination (ρ = 30 mW/cm^2) and (b) without lighting.

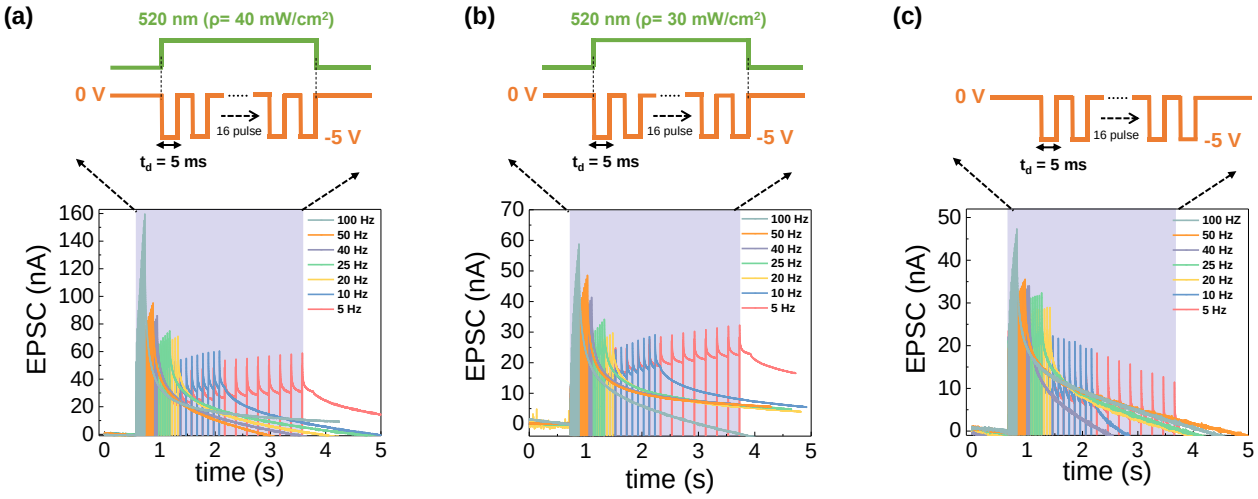

Figure S13. SRDP of the ZTO/Au NPs optosynaptic transistor with the application of voltage spikes (V_G = -5 V, t_d = 5 ms, N = 16) under 520 nm light illumination with (a) ρ = 40 mW/cm^2, (b) ρ = 30 mW/cm^2, and (c) without lighting.

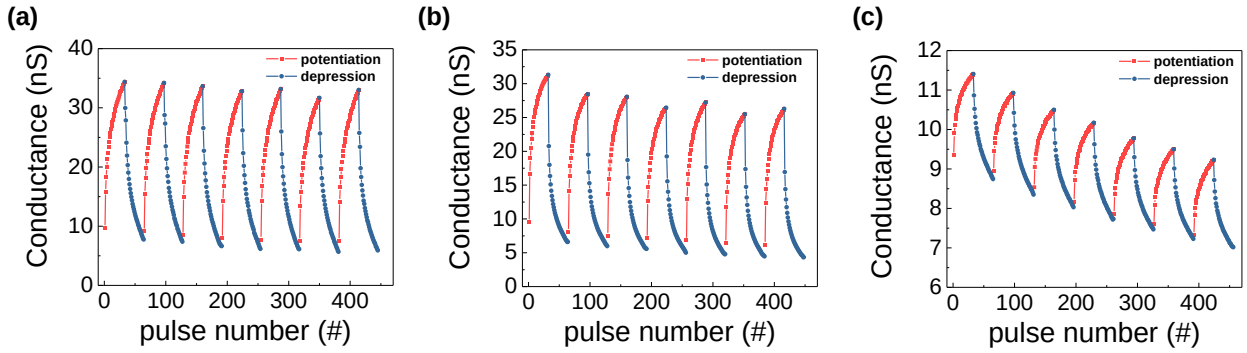

Figure S14. The cycled LTP/LTD characteristics of the ZTO/Au NPs optosynaptic transistor with potential spikes of **(**a) V_G = -5 V (t_d = 5 ms, 10 ms period) under 520 nm light illumination, (b) V_G = -5 V (t_d = 100 ms, 200 ms period) without lighting, and (c) V_G = -5 V (t_d = 5 ms, 10 ms period) without lighting. The same depression spikes of V_G = 1.2 V (t_d = 5 ms, 10 ms period) without lighting for depression in three cases.

Table S1. Statistical analysis of mean value (μ) and standard deviation (σ) on the extracted electrical characteristics of ZTO/Au NPs phototransistors measured in the dark. (See Fig. S11b-e)

Electrical characteristics	**μ**	**σ**	**Coefficient of variation (%)**
Electron mobility (cm^2/Vs)	0.44	0.05	10.78%
On/off current ratio	2.49×10^7	1.49×10^7	59.82%
Subthreshold swing (V/decade)	1.31	0.28	21.29%
Turn-on voltage (V)	-6.23	0.42	-6.70%

Table S2. Statistical analysis of mean value (μ), standard deviation (σ), and coefficient of variation on the photoresponsivity of the ZTO/Au NPs phototransistors to 520 nm light. (See Fig. S11f)

Optical power density	**μ (A/W)**	**σ (A/W)**	**Coefficient of variation (%)**
$\rho = 20\ mW/cm^2$	1.15	0.03	2.86%
$\rho = 30\ mW/cm^2$	0.83	0.03	3.46%
$\rho = 40\ mW/cm^2$	0.69	0.03	4.71%
$\rho = 50\ mW/cm^2$	0.61	0.03	4.69%

Table S3. Extracted fitting parameters from Fig. S14 using eq. (3) and (4).

Excitatory stimuli	α_P	α_D	β_P	β_D	G_{max}	G_{min}	G_{max}/ G_{min}
V_G = -5 V (t_d = 5 ms) under lighting	6.0×10^{-9}	5.08×10^{-9}	3.42	3.15	34.3 nS	9.7 nS	3.5
V_G = -5 V (t_d = 100 ms) without lighting	7.17×10^{-9}	1.06×10^{-8}	3.57	3.74	31.3 nS	9.5 nS	3.3
V_G = -5 V (t_d = 100 ms) without lighting	5.46×10^{-10}	5.55×10^{-10}	3.54	3.08	11.4 nS	9.3 nS	1.2

Table S4. Comparison of the performances of optoelectronic synaptic transistors reported in the literature with those of our work.

Device Structure	Potentiation/depression	Pulse width	G_{max}/G_{min}	Energy Consumption
Pentacene/ $MoSe_2/Bi_2Se_3$/PMMA[S1]	Potentiation: 790 nm Depression: V_G = -10 V	Potentiation: 10 ms Depression: 1 ms	~1.4	3 nJ
Pentacene/PMMA/Zr-$CsPbI_3$ perovskite[S2]	Potentiation: 405 nm Depression: V_G = -40 V	Potentiation: 0.1 s Depression: 1.5 s	~4	~8 μJ
VO_2[S3]	Potentiation: UV Depression: V_G = −1.5 increase to −3.5 V	Potentiation: 10 s Depression: 10 s	~1.8	11 nJ
IGZO[S4]	Potentiation: UV Depression: V_G = 8 V	Potentiation: 100 ms Depression: 100 ms	~1.4	2 μJ
IGZO[S5]	Potentiation: 470 nm Depression: V_G = 0.05 increase to 1 V	Potentiation: 400 ms Depression: 400 ms	~36.6	64 μJ
β-Ga_2O_3[S6]	Potentiation: UV Depression: V_G = 50 V	Potentiation: 500 ms Depression: 500 ms	~3.5	500 nJ
ZTO/Au NPs heterostructure[this work]	Potentiation: V_G = -5 V under 520 nm lighting Depression: V_G = 1.2 V	Potentiation: 5 ms Depression: 5 ms	~3.5	17 nJ

References

S1 Y. Wang, J. Yang, W. Ye, D. She, J. Chen, Z. Lv, V. A. L. Roy, H. Li, K. Zhou, Q. Yang, Y. Zhou and S. T. Han, *Adv. Electron. Mater.*, 2019, **6**, 1900765.

S2 H. Shao, Y. Li, W. Yang, X. He, L. Wang, J. Fu, M. Fu, H. Ling, P. Gkoupidenis, F. Yan, L. Xie and W. Huang, *Adv. Mater.*, 2023, **35**, e2208497.

S3 G. Li, D. Xie, H. Zhong, Z. Zhang, X. Fu, Q. Zhou, Q. Li, H. Ni, J. Wang, E. J. Guo, M. He, C. Wang, G. Yang, K. Jin and C. Ge, *Nat. Commun.*, 2022, **13**, 1729.

S4 N. Duan, Y. Li, H. C. Chiang, J. Chen, W. Q. Pan, Y. X. Zhou, Y. C. Chien, Y. H. He, K. H. Xue, G. Liu, T. C. Chang and X. S. Miao, *Nanoscale*, 2019, **11**, 17590-17599.

S5 Y. Li, T. Chen, X. Ju and T. Salim, *Nanoscale*, 2022, **14**, 10245-10254.

S6 Y. Yoon, Y. Kim, W. S. Hwang and M. Shin, *Adv. Electron. Mater.*, 2023, **9**, 2300098.